



## Distribution and Pharmacokinetics of the Prodrug Daunorubicin-GA3 in Nude Mice Bearing Human Ovarian Cancer Xenografts

Pieter H. J. Houba,\* Epie Boven,\* Ida H. van der Meulen-Muileman,\*  
Ruben G. G. Leenders,† Johannes W. Scheeren,† Herbert M. Pinedo\*  
and Hidde J. Haisma\*‡

\*DEPARTMENT OF MEDICAL ONCOLOGY, UNIVERSITY HOSPITAL VRIJE UNIVERSITEIT, AMSTERDAM; AND

†DEPARTMENT OF ORGANIC CHEMISTRY, UNIVERSITY OF NIJMEGEN, NIJMEGEN, THE NETHERLANDS

**ABSTRACT.** *N*-[4-daunorubicin-*N*-carbonyl (oxymethyl)phenyl] *O*- $\beta$ -glucuronyl carbamate (DNR-GA3) is a glucuronide prodrug of daunorubicin (DNR) which induced a better tumor growth delay than DNR when studied at equitoxic doses in three human ovarian cancer xenografts. These results suggested that the prodrug DNR-GA3 was selectively activated by human  $\beta$ -glucuronidase present in tumor tissue. We determined the pharmacokinetics and distribution of DNR-GA3 in nude mice bearing human ovarian cancer xenografts (OVCAR-3, FMa, A2780, and MRI-H-207). Administration of DNR at 10 mg/kg i.v. (maximum tolerated dose) to OVCAR-3-bearing mice resulted in a peak plasma concentration of the drug of 12.18  $\mu$ M ( $t = 1$  min). DNR-GA3 at 100 mg/kg i.v. (approximately 50% of the maximum tolerated dose [MTD]) resulted in a peak plasma concentration of DNR that was 28-fold lower than that after DNR itself; in normal tissues, prodrug injection resulted in 5- to 23-fold lower DNR concentrations. DNR showed a relatively poor uptake into OVCAR-3 tumors with a peak concentration of 2.05 nmol  $\cdot$  g<sup>-1</sup> after injection. In the same xenograft, DNR-GA3 resulted in a significantly higher DNR peak concentration of 3.45 nmol  $\cdot$  g<sup>-1</sup> ( $P < 0.05$ ). The higher area under the curve of DNR in tumor tissue after DNR-GA3 than after DNR itself would be the result of prodrug activation by  $\beta$ -glucuronidase. In this respect, a considerably higher  $\beta$ -glucuronidase activity was found in tumor tissue when compared to plasma. The specific activation of DNR-GA3 by  $\beta$ -glucuronidase at the tumor site relative to normal organs leads to a more tumor-selective therapy, resulting in greater efficacy without increased toxicity. *BIOCHEM PHARMACOL* 57;6:673–680, 1999. © 1999 Elsevier Science Inc.

**KEY WORDS.** anthracycline prodrugs; daunorubicin; human  $\beta$ -glucuronidase; human ovarian cancer xenografts

Anthracyclines, with DOX§ and DNR as important representatives, are effective anticancer agents used in the treatment of leukemias, lymphomas, and a number of solid tumor types. Cumulative dose-related cardiotoxicity, however, is a major side-effect of these compounds, in addition to acute toxicities such as myelosuppression, nausea, and vomiting. Reduction of the toxicities associated with anthracyclines and retention of their activity remain a challenge in the field of cancer chemotherapy.

For many years, efforts have been made to improve the selectivity and efficacy of chemotherapy using non-toxic prodrugs that are preferentially converted into active anti-

cancer agents at the tumor site [1]. An example of such a prodrug is peptidyl-doxorubicin, which is activated by plasmin that is present in a higher concentration in tumor tissue [2]. This prodrug was not developed further, because the activation rate was too slow for *in vivo* efficacy. *N*-*L*-leucyl-DOX is a prodrug of DOX which is activated by tumor peptidases [3]. In human ovarian cancer xenografts, *N*-*L*-leucyl-DOX was demonstrated to be more effective than DOX [4]. Clinical studies on *N*-*L*-leucyl-DOX have indicated premature activation of the prodrug in the circulation, possibly reducing the selectivity of the prodrug [5].

We have previously shown *in vitro* that glucuronide derivatives of anthracyclines, such as epirubicin-glucuronide [6] and daunorubicin-glucuronides [7, 8], are stable in physiological buffer and plasma. They are relatively non-toxic and can only be activated to the active anthracycline by  $\beta$ -glucuronidase. The glucuronide-anthracyclines were found to be highly hydrophilic, which impairs their ability to enter cells. DNR-GA3 (Fig. 1) is a derivative of DNR in which the glucuronic acid moiety is linked to the anthra-

‡ Corresponding author: H. J. Haisma, Ph.D., Department of Medical Oncology, University Hospital Vrije Universiteit, P.O. Box 7057, 1007 MB Amsterdam, The Netherlands. Tel. +31 20 444 4300; FAX +31 20 444 4355; E-mail: HJ.Haisma.Oncol@med.vu.nl

§ Abbreviations: AUC, area under the concentration–time curve; DNR, daunorubicin; DNR-GA3, *N*-[4-daunorubicin-*N*-carbonyl (oxymethyl)phenyl] *O*- $\beta$ -glucuronyl carbamate; DOX, doxorubicin; DTI, drug targeting index; saccharolactone, D-glucaric acid-1,4-lactone monohydrate; and MTD, maximum tolerated dose.

Received 24 April 1998; accepted 8 September 1998.

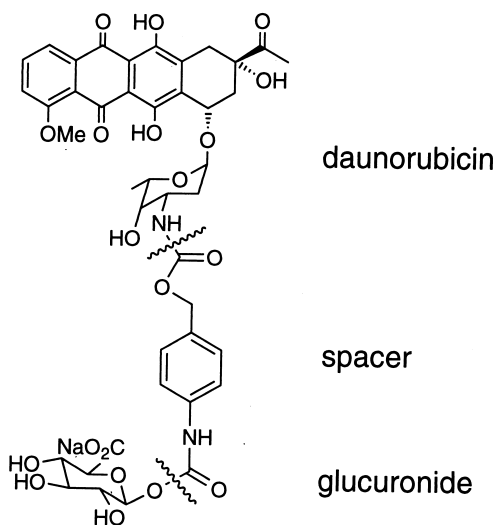


FIG. 1. Chemical structure of prodrug N[4-daunorubicin-N-carbonyl (oxymethyl) phenyl] O-β-glucuronyl carbamate (DNR-GA3).

cycline via a synthetic spacer.\* DNR-GA3 treatment induced an improved tumor growth delay when compared with equitoxic doses of DNR in three human ovarian cancer xenografts (OVCAR-3, A2780, MRI-H-207) which were sensitive to DNR [10]. These results suggested that the prodrug DNR-GA3 was selectively activated by human β-glucuronidase present in tumor tissue.

In the present experiments, we wished to determine whether DNR-GA3 was specifically activated to DNR in tumor tissue. As a model we used four different human ovarian cancer xenografts grown subcutaneously (s.c.) in nude mice. The pharmacokinetics and distribution of DNR and DNR-GA3 were measured not only in tumor tissue, but also in plasma and normal mouse organs. As the generation of DNR from the prodrug is mediated by β-glucuronidase, enzyme activity levels in plasma and tumor tissue were determined. We demonstrated that DNR-GA3 has a higher therapeutic index than DNR on the basis of 1) the specific activation of DNR-GA3 by β-glucuronidase at the tumor site relative to normal organs, and 2) higher DNR concentrations in tumor tissue after injection of DNR-GA3 than after DNR administration when the drugs are given at equitoxic doses.

## MATERIALS AND METHODS

### Materials

Daunorubicin (DNR, Société Parisienne d'expansion chimique) was purchased as a powder. The prodrug DNR-GA3 has been characterized [7, \*]. In this prodrug the anthracycline moiety is linked to the glucuronide via a carbamate spacer with an aromatic center. Stock solutions of DNR and DNR-GA3 were prepared in sterile water and stored at  $-20^{\circ}$ .

### Tumor Models

Female athymic nude mice (Hsd: athymic nude-*nu*; Harlan Cpb) were handled under specified pathogen-free conditions. The human ovarian cancer xenografts OVCAR-3, FMa, A2780, and MRI-H-207 have been described earlier [10]. The OVCAR-3 xenograft is a poorly differentiated serous adenocarcinoma with a mean volume doubling time of 5.5 days. The FMa xenograft is a poorly differentiated mucinous adenocarcinoma with a mean volume doubling time of 6.0 days. The A2780 and MRI-H-207 xenografts are undifferentiated carcinomas both having a mean volume doubling time of 3.0 days. Tumors from previous recipients were transferred by implanting tissue fragments with a diameter of 2–3 mm into both flanks of 8-to-10-week-old mice. Upon growth, tumors were measured by the same observer. The tumor volume was calculated by the equation length  $\times$  width  $\times$  thickness  $\times$  0.5, and expressed in  $\text{mm}^3$ .

Control and treatment groups consisted of 6 animals each. Treatment was started when the mean tumor volume was approximately  $150 \text{ mm}^3$ . Drug doses were selected to be equitoxic on the basis of weight loss; a reversible loss was required of approximately 10% of the initial weight within 2 weeks after the first injection. DNR was given in a dose of 8–10 mg/kg i.v. weekly  $\times$  2 to mice. DNR-GA3 was studied at a dose of 150–250 mg/kg i.v. given once. Mice were weighed twice a week and tumors were measured on the same days [9]. The relative tumor volume was expressed by the formula  $V_T/V_0$ , where  $V_T$  is the volume on any given day and  $V_0$  is the volume on day 0. The ratio between the mean of the relative volumes of treated tumors and that of control tumors  $\times$  100% (T/C%) was assessed on each day of measurement, and the optimal ratio was used to calculate the GI% (GI% = 100% - T/C%). The efficacy of the different treatments is depicted in Table 1.

### Distribution of DNR and DNR-GA3 in Tumor and Normal Tissues

Nude mice bearing s.c. xenografts with a mean volume of  $600 \text{ mm}^3$  were injected i.v. with DNR 10 mg/kg (OVCAR-3) or DNR-GA3 100 mg/kg (OVCAR-3, FMa, A2780, MRI-H-207). Because of the limited availability of DNR-GA3, we investigated DNR-GA3 at approximately half of the MTD. At different time points ranging from 1 min to 48 hr, blood, tumors, liver, heart, and kidneys were removed in groups of three OVCAR-3-bearing mice per time point. The animals with other xenografts received DNR-GA3 only and (pro)drug concentrations were determined in plasma and tumor tissue. Blood was collected in heparinized vials and centrifuged at  $16,000 \text{ g}$  for 5 min. To plasma, 1/100 volume of 100 mM saccharolactone (Fluka) was added to prevent hydrolysis of DNR-GA3 by β-glucuronidase. Saccharolactone is a selective competitive inhibitor of β-glucuronidase which completely abolishes the activity of the latter at the concentration used (1 mM). Samples were stored at  $-20^{\circ}$ . For analysis of anthracy-

\*Leenders RGG, Damen EWP, Bijsterveld EJA, Scheeren JW, Houba PHJ, Boven E and Haisma HJ, submitted for publication.

TABLE 1. Treatment with DNR or DNR-GA3 in mice bearing human ovarian cancer xenografts\*

Xenograft	Histology	Treatment	Dose i.v. (mg/ kg)	Days	GI%†
OVCAR-3	Poorly differentiated serous	DNR	10	0, 7	47
		DNR-GA3	250	0	82
FMa	Poorly differentiated mucinous	DNR	8	0, 7	0
		DNR-GA3	250	0	24
A2780	Undifferentiated	DNR	8	0, 7	41
		DNR-GA3	150	0	86
MRI-H-207	Undifferentiated	DNR	8	0, 7	40
		DNR-GA3	200	0	95

\* [9].

† Maximum growth inhibition with reference to untreated tumors.

cline contents in the plasma samples, plasma (10  $\mu\text{L}$ ) was diluted in ice-cold methanol (140  $\mu\text{L}$ ), incubated at  $-20^\circ$  for at least 10 min, and centrifuged (16,000 g, 5 min). To the supernatant (100  $\mu\text{L}$ ) 12 mM  $\text{H}_3\text{PO}_4$  (25  $\mu\text{L}$ ) was added. Samples were stored at  $-20^\circ$  until HPLC analysis.

Tumor, liver, heart, and kidney tissues were immediately frozen in liquid nitrogen and stored at  $-20^\circ$  until preparation for HPLC analysis. Tissue samples were diluted (230 mg tissue/770  $\mu\text{L}$  buffer) in 20 mM  $\text{H}_3\text{PO}_4$ /1 mM saccharolactone (pH 3.0,  $0^\circ$ ) and homogenized (1 min, 4000 rpm,  $0^\circ$ ) using a polytron. The homogenate (200  $\mu\text{L}$ ) was diluted in 3.3% (w/v)  $\text{AgNO}_3$  (40  $\mu\text{L}$ ) and acetonitrile (160  $\mu\text{L}$ ), shaken (15 min, room temperature), sonicated (15 min, room temperature) and centrifuged (16,000 g, 5 min). The supernatant (100  $\mu\text{L}$ ) was diluted in ice-cold methanol (600  $\mu\text{L}$ ), incubated at  $-20^\circ$  for at least 10 min, and centrifuged (16,000 g, 5 min). The supernatant was stored at  $-20^\circ$  until reversed-phase HPLC analysis.

### HPLC Analysis

The HPLC apparatus consisted of an autosampler (Marathon-XT), a pump (Separations, Model 300), and a fluorescence detector (Jasco, Model 821-FP: excitation 480 nm; emission 580 nm). For analysis of anthracycline contents in the tissues and plasma, 50- $\mu\text{L}$  samples were loaded on a reversed-phase column (Chromsep  $\text{C}_{18}$ ,  $2 \times 100 \text{ mm} \times 4.6 \text{ mm}$ , 3  $\mu\text{m}$  particle size). Elution was done with eluents in an isocratic run (0.5 mM triethylamine/20 mM sodium phosphate, adjusted to pH 4.0 with 1 M  $\text{H}_3\text{PO}_4$ ; acetonitrile = 2:1). In each cluster of runs, standards of DNR-GA3, DNR, and daunorubicinol were included, at the beginning and at the end of the cluster. The elution peaks in the chromatograms were integrated using the GyncoSoft program (GynkoteK, Version 5.3E). Calibration of the system was performed as described [11] and the detection limit was 0.01  $\mu\text{M}$  (pro)drug.

Data were analyzed with the Topfit software program in order to calculate half-life times and AUCs. Differences in drug concentrations per time point were evaluated with the Student's *t*-test.

### $\beta$ -Glucuronidase Activity in Plasma and Tumor Tissue

From OVCAR-3, FMa, A2780, MRI-H-207, and control mice, blood samples were collected from the eye plexus using heparinized glass capillaries and plasma was prepared. From the tumor-bearing mice, the tumors were removed and immediately frozen in liquid nitrogen and stored at  $-20^\circ$  until sample preparation. Tumor tissue was homogenized in phosphate-buffered saline (230 mg/mL) for 1 min at 4000 rpm at  $0^\circ$  using a polytron. The  $\beta$ -glucuronidase activity in plasma and tumor homogenate was determined with 4-methylumbelliferyl- $\beta$ -D-glucuronide (5 mM) at pH 4.2 and  $37^\circ$  as described [12], and fluorescence values were converted to units using a specific activity for  $\beta$ -glucuronidase of 30 U/mg [7].

## RESULTS

### Pharmacokinetics in Plasma

Administration of DNR to OVCAR-3-bearing mice resulted in a peak concentration of the drug of 12.18  $\mu\text{M}$  ( $t = 1 \text{ min}$ ) in plasma and an elimination half-life time of 49 min. After administration of DNR-GA3 to OVCAR-3-bearing mice, the prodrug reached a plasma peak concentration of 390  $\mu\text{M}$  ( $t = 1 \text{ min}$ ; Fig. 2) and was eliminated with a half-life time of 17 min. DNR-GA3 administration resulted in a peak plasma concentration of DNR that was 28-fold lower than that after DNR administration itself, reaching a maximum value of 0.43  $\mu\text{M}$  ( $t = 1 \text{ min}$ ) with an elimination half-life time of 32 min. In the other xenografts (FMa, A2780, MRI-H-207), peak plasma concentrations of DNR-GA3 ranged from 350–800  $\mu\text{M}$  ( $t = 1 \text{ min}$ ), and concentrations of DNR peaked at 30 min and ranged from 0.27–0.70  $\mu\text{M}$  (Table 2).

### Distribution and Kinetics in Normal Tissues

The distribution of DNR and DNR-GA3 in normal tissues was compared in OVCAR-3-bearing mice (Table 2). After administration of DNR, peak concentrations were detected at 1 min after injection. The highest concentration was measured in kidney (120.54  $\text{nmol} \cdot \text{g}^{-1}$ ) followed by liver

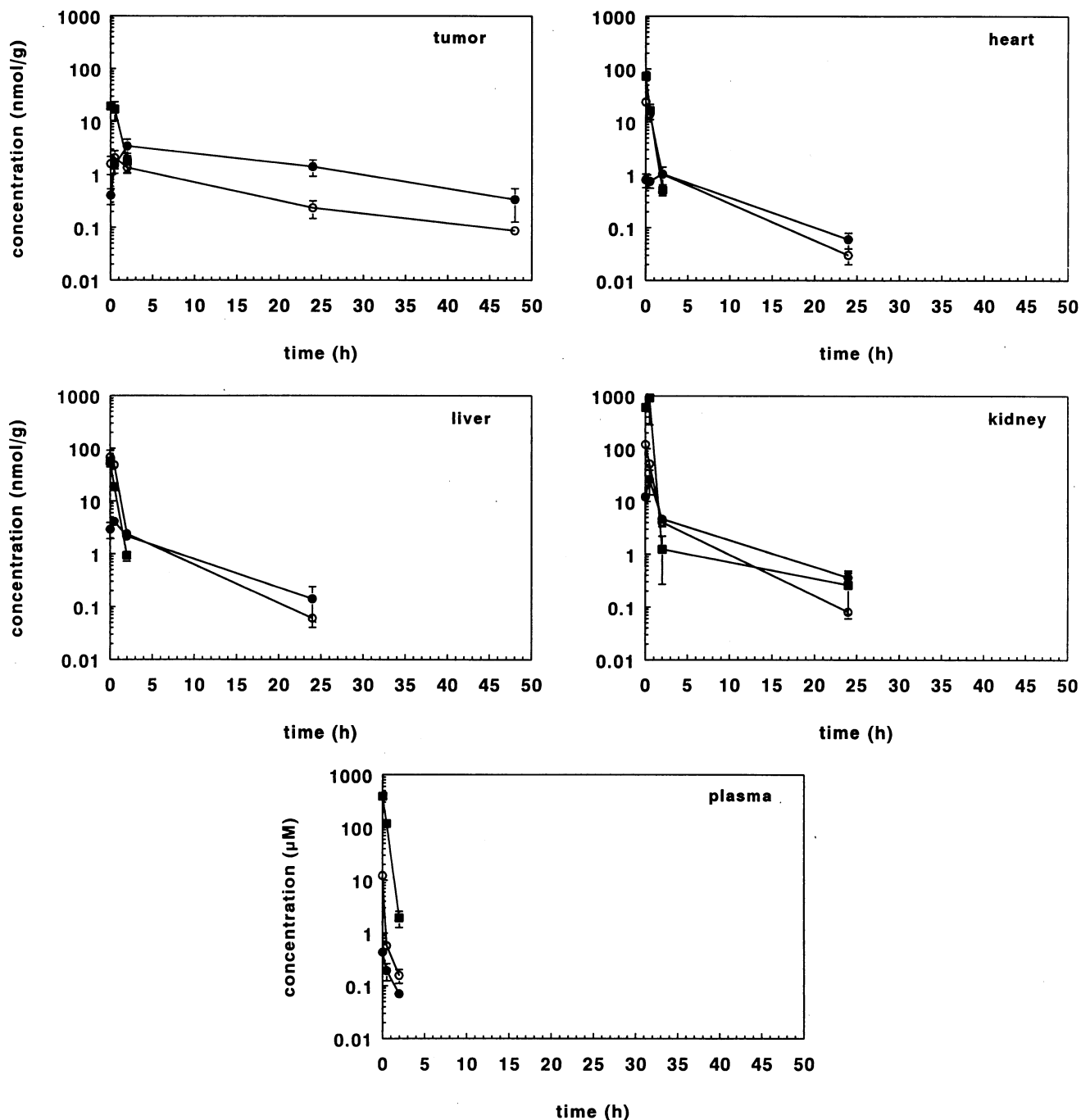


FIG. 2. The concentration–time curves of: DNR (○) as a result of the administration of 10 mg/kg DNR; DNR (●) as a result of the administration of 100 mg/kg DNR-GA3; and DNR-GA3 (■) after 100 mg/kg DNR-GA3 in plasma, tumors, liver, heart, and kidneys of OVCAR-3-bearing mice. Bars,  $\pm$  SD.

(68.17  $\text{nmol} \cdot \text{g}^{-1}$ ) and heart (23.61  $\text{nmol} \cdot \text{g}^{-1}$ ). After DNR-GA3 administration to OVCAR-3-bearing mice, peak concentrations of DNR-GA3 were highest in kidney (911.7  $\text{nmol} \cdot \text{g}^{-1}$ ,  $t = 30$  min) followed by heart (72.68  $\text{nmol} \cdot \text{g}^{-1}$ ,  $t = 1$  min) and liver (56.70  $\text{nmol} \cdot \text{g}^{-1}$ ,  $t = 1$  min). Prodrug injection resulted in 5- to 23-fold lower DNR concentrations in these tissues, with peak concentrations of 26.11  $\text{nmol} \cdot \text{g}^{-1}$  (kidney), 4.07  $\text{nmol} \cdot \text{g}^{-1}$  (liver), and 1.03  $\text{nmol} \cdot \text{g}^{-1}$  (heart), at 30 min to 2 hr after injection of the

prodrug. DNR concentrations after prodrug or drug administration at 2 hr after injection were not significantly different (Fig. 3).

#### Distribution and Kinetics in Tumor Tissue

Administration of DNR to OVCAR-3-bearing mice resulted in a peak concentration of the drug in OVCAR-3 tumor tissue of 2.05  $\text{nmol} \cdot \text{g}^{-1}$  at 30 min after injection

**TABLE 2.** Daunorubicin concentrations in plasma and tissues of tumor-bearing nude mice after i.v. administration of DNR (10 mg/kg) or DNR-GA3 (100 mg/kg)

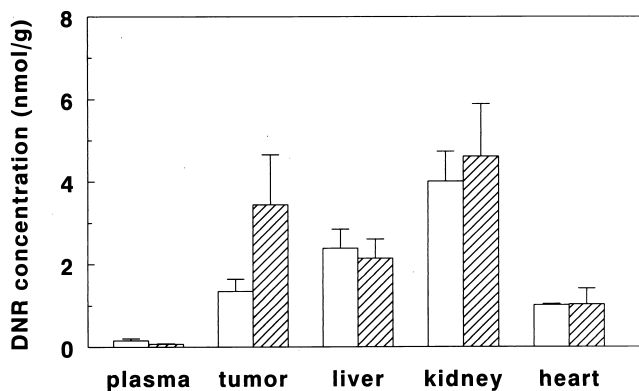
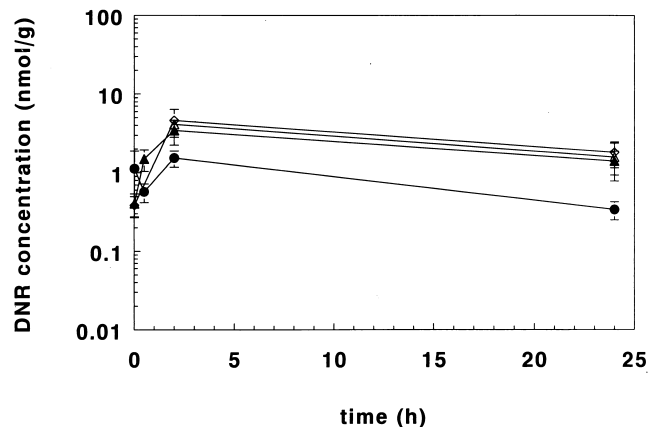
Group	Treatment	Time point	Plasma $\mu\text{M} \pm \text{SD}$	Tumor $\text{nmol} \cdot \text{g}^{-1} \pm \text{SD}$	Liver $\text{nmol} \cdot \text{g}^{-1} \pm \text{SD}$	Heart $\text{nmol} \cdot \text{g}^{-1} \pm \text{SD}$	Kidney $\text{nmol} \cdot \text{g}^{-1} \pm \text{SD}$
OVCAR-3	DNR	1 min	12.18 $\pm$ 2.09	1.59 $\pm$ 0.60	68.17 $\pm$ 9.26	23.61 $\pm$ 5.07	120.54 $\pm$ 15.10
OVCAR-3	DNR-GA3	1 min	0.43 $\pm$ 0.04*	0.40 $\pm$ 0.14*	2.91 $\pm$ 0.98*	0.80 $\pm$ 0.23*	12.16 $\pm$ 2.41*
FMa	DNR-GA3	1 min	0.23 $\pm$ 0.04	0.38 $\pm$ 0.11	ND	ND	ND
A2780	DNR-GA3	1 min	0.17 $\pm$ 0.06	1.12 $\pm$ 0.76	ND	ND	ND
MRI-H-207	DNR-GA3	1 min	0.19 $\pm$ 0.03	<0.01	ND	ND	ND
OVCAR-3	DNR	30 min	0.57 $\pm$ 0.03	2.05 $\pm$ 0.78	48.09 $\pm$ 0.85	13.92 $\pm$ 2.42	51.36 $\pm$ 2.55
OVCAR-3	DNR-GA3	30 min	0.19 $\pm$ 0.07*	1.49 $\pm$ 0.45	4.07 $\pm$ 0.78*	0.75 $\pm$ 0.19*	26.11 $\pm$ 12.80*
FMa	DNR-GA3	30 min	0.70 $\pm$ 0.29	ND	ND	ND	ND
A2780	DNR-GA3	30 min	0.27 $\pm$ 0.06	0.57 $\pm$ 0.15	ND	ND	ND
MRI-H-207	DNR-GA3	30 min	0.48 $\pm$ 0.08	ND	ND	ND	ND
OVCAR-3	DNR	2 hr	0.16 $\pm$ 0.05	1.34 $\pm$ 0.30	2.39 $\pm$ 0.46	1.02 $\pm$ 0.03	4.01 $\pm$ 0.72
OVCAR-3	DNR-GA3	2 hr	0.07 $\pm$ 0.01*	3.45 $\pm$ 1.21*	2.15 $\pm$ 0.46	1.03 $\pm$ 0.38	4.61 $\pm$ 1.28
FMa	DNR-GA3	2 hr	0.28 $\pm$ 0.06	4.61 $\pm$ 1.78	ND	ND	ND
A2780	DNR-GA3	2 hr	0.12 $\pm$ 0.04	1.53 $\pm$ 0.36	ND	ND	ND
MRI-H-207	DNR-GA3	2 hr	0.08 $\pm$ 0.02	4.12 $\pm$ 0.65	ND	ND	ND
OVCAR-3	DNR	24 hr	<0.01	0.23 $\pm$ 0.09	0.06 $\pm$ 0.01	0.03 $\pm$ 0.01	0.08 $\pm$ 0.02
OVCAR-3	DNR-GA3	24 hr	<0.01	1.40 $\pm$ 0.47*	0.14 $\pm$ 0.10	0.06 $\pm$ 0.02	0.36 $\pm$ 0.12*
FMa	DNR-GA3	24 hr	<0.01	1.80 $\pm$ 0.65	ND	ND	ND
A2780	DNR-GA3	24 hr	<0.01	0.34 $\pm$ 0.09	ND	ND	ND
MRI-H-207	DNR-GA3	24 hr	<0.01	1.57 $\pm$ 0.79	ND	ND	ND
OVCAR-3	DNR	48 hr	<0.01	0.09	ND	ND	ND
OVCAR-3	DNR-GA3	48 hr	<0.01	0.34 $\pm$ 0.21	ND	ND	ND
FMa	DNR-GA3	48 hr	ND	ND	ND	ND	ND
A2780	DNR-GA3	48 hr	<0.01	0.16 $\pm$ 0.15	ND	ND	ND
MRI-H-207	DNR-GA3	48 hr	ND	ND	ND	ND	ND

\* $P < 0.05$  when compared with DNR treatment.

†ND, not determined.

(Table 2; Fig. 2) and an elimination half-life time = 460 min. In the same tumor model, administration of the prodrug DNR-GA3 resulted in a peak concentration of DNR-GA3 of 19.7  $\text{nmol} \cdot \text{g}^{-1}$  ( $t = 1$  min). DNR-GA3 was rapidly cleared from the tumor (Fig. 2). A significantly higher ( $P < 0.002$ ) DNR peak concentration of 3.45  $\text{nmol} \cdot \text{g}^{-1}$  was found at 2 hr after prodrug injection. Figure 3 illustrates the higher DNR concentration that was reached in the OVCAR-3 tumor as a result of DNR-GA3 administration. An elimination half-life time for DNR from

DNR-GA3 of 660 min was calculated. In the other three xenografts, the prodrug reached peak concentrations ranging from 17.1  $\text{nmol} \cdot \text{g}^{-1}$  to 36.3  $\text{nmol} \cdot \text{g}^{-1}$  at 1 min after administration. DNR-GA3 itself was again rapidly cleared, irrespective of the tumor model. Tumor DNR concentrations were maximal at 2 hr after injection of the prodrug and ranged from 1.53 to 4.61  $\text{nmol} \cdot \text{g}^{-1}$  (Table 2), with an elimination half-life time of 660 min for all three xenografts as illustrated in Fig. 4.

**FIG. 3.** The concentration of DNR as a result of 10 mg/kg DNR (closed bars) or 100 mg/kg DNR-GA3 (hatched bars) at 2 hr after administration to OVCAR-3-bearing nude mice expressed for plasma in  $\mu\text{M}$  and for tissues in  $\text{nmol} \cdot \text{g}^{-1}$ . Bars,  $\pm$  SD.**FIG. 4.** The concentration-time curves of DNR in the four ovarian cancer xenografts after DNR-GA3 administration (100 mg/kg).  $\blacktriangle$ , OVCAR-3;  $\diamond$ , FMa;  $\bullet$ , A2780;  $\triangle$ , MRI-H-207. Bars,  $\pm$  SD.

**TABLE 3.** AUC of daunorubicin in plasma and tissues of tumor-bearing mice after i.v. administration of DNR (10 mg/kg) or DNR-GA3 (100 mg/kg)

Group	Treatment	Plasma ( $\mu\text{mol} \cdot \text{min}^{-1} \cdot \text{mL}^{-1}$ )	Tumor ( $\mu\text{mol} \cdot \text{min}^{-1} \cdot \text{g}^{-1}$ )	Liver ( $\mu\text{mol} \cdot \text{min}^{-1} \cdot \text{g}^{-1}$ )	Heart ( $\mu\text{mol} \cdot \text{min}^{-1} \cdot \text{g}^{-1}$ )	Kidney ( $\mu\text{mol} \cdot \text{min}^{-1} \cdot \text{g}^{-1}$ )
OVCAR-3	DNR	0.217	1.48	5.57	1.91	7.68
OVCAR-3	DNR-GA3	0.009	4.70	1.89	0.82	5.22
FMa	DNR-GA3	0.058	4.53	ND*	ND	ND
A2780	DNR-GA3	0.024	1.72	ND	ND	ND
MRI-H-207	DNR-GA3	0.035	4.00	ND	ND	ND

\*ND, not determined.

### Formation of Daunorubicinol

Daunorubicinol is the major metabolite of DNR and has approximately 10% of the antitumor activity of DNR *in vitro* [13]. Daunorubicinol could have contributed to the observed growth inhibition induced by DNR or DNR-GA3. Therefore, daunorubicinol concentrations were compared at 2 hr after administration in OVCAR-3-bearing mice, when the highest drug concentrations were found in tumor tissues (Table 2). No significant difference was found between the ratios of DNR and daunorubicinol after administration of DNR or DNR-GA3 in the plasma (0.52 and 0.55, respectively) or in tumor tissue (0.29 and 0.26, respectively).

### Areas under the Concentration versus Time Curve (AUC)

The AUC of DNR was calculated for plasma, normal mouse organs, and OVCAR-3 tumor tissue by the trapezoidal rule using the available data and the Topfit software program (Table 3). The plasma AUC of DNR after administration of DNR ( $0.217 \mu\text{mol} \cdot \text{min}^{-1} \cdot \text{mL}^{-1}$ ) was considerably higher than that after injection of DNR-GA3 ( $0.009 \mu\text{mol} \cdot \text{min}^{-1} \cdot \text{mL}^{-1}$ ). For the liver, heart, and kidney, the respective DNR AUCs were 3.0-, 2.3-, and 1.5-fold higher after DNR than after prodrug administration. The reverse was observed in OVCAR-3 tumor tissue, where the AUC of DNR from DNR-GA3 was 3-fold higher than that after DNR. In the other xenografts, the AUCs of DNR from DNR-GA3 in plasma and tumor tissues were comparable to those found in OVCAR-3-bearing mice, except for the lower AUC of DNR from DNR-GA3 in A2780 tumor tissue.

### Drug Targeting Index (DTI)

The efficiency of targeting can be described as a drug targeting index [14]. Assuming that the AUCs at the response (tumor) and toxic sites (bone marrow, heart) reflect the relative activity and toxicity of the drug, DTI can be defined as follows:

$$\text{DTI} = \frac{\text{AUC (R, target)/AUC (T, target)}}{\text{AUC (R, non-target)/AUC (T, non-target)}}$$

where R represents the response site (tumor) and T the toxic site after targeted delivery (DNR-GA3, target) and non-targeted delivery (DNR, non-target), respectively. A value higher than 1 indicates targeting to the response site. We calculated the DTI for plasma (as a surrogate for bone marrow) and heart tissue, because these are the major organs for anthracycline toxicity. For plasma, a high DTI of 77 was calculated, whereas the DTI for heart tissue was 7.4. Significantly, these values were calculated from the data obtained after administration of DNR at 10 mg/kg (the MTD) and of DNR-GA3 at 100 mg/kg (50% of the MTD). If the formation of DNR from DNR-GA3 shows linear pharmacokinetics, these values will be more pronounced when the prodrug is given at the MTD.

### $\beta$ -Glucuronidase Activity in Plasma and Tumor Tissue

The prodrug DNR-GA3 is activated to the active drug DNR by  $\beta$ -glucuronidase. In order to determine if there was a correlation between the enzyme activity in the tumor, the DNR-GA3 activation, and the antitumor response, the  $\beta$ -glucuronidase concentration was measured in the tumors and plasma of the tumor-bearing mice. The enzyme activity in plasma was very low, ranging from 135–201 nU/mL plasma, and was similar to the levels found in control nude mice. The enzyme activity in the tumor homogenates was 170–1000 times higher than that in plasma and varied between the four xenografts (Fig. 5). The enzyme activity was highest in the OVCAR-3 tumors and lowest in the A2780 tumors. No relation was found between the  $\beta$ -glucuronidase activity in tumor tissue and the AUC of DNR from DNR-GA3 administration.

### DISCUSSION

Earlier we observed that inhibition of tumor growth caused by DNR-GA3 was superior to the antitumor effects of equitoxic doses of DNR in three of four human ovarian cancer xenografts. We have now demonstrated that this better tumor growth-inhibiting effect was caused by the specific activation of DNR-GA3 by  $\beta$ -glucuronidase at the tumor site. This led to higher concentrations of DNR in tumor tissue after administration of DNR-GA3, while in plasma and normal tissues the concentrations of DNR were

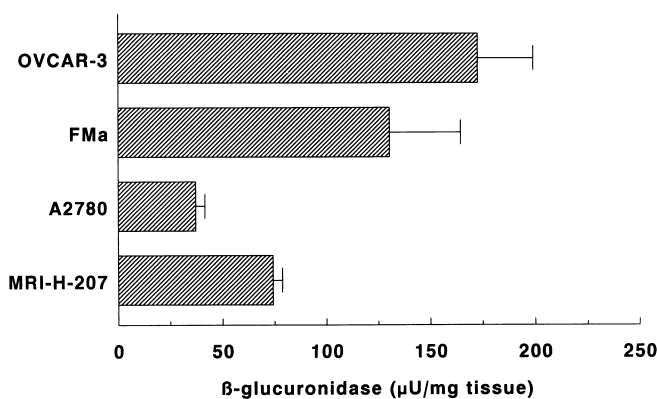


FIG. 5.  $\beta$ -Glucuronidase activity in homogenates of OVCAR-3, FMa, A2780, or MRI-H-207 xenografts. Bars,  $\pm$ SD.

lower when compared with the DNR values after DNR injection. A favorable DTI was calculated for DNR-GA3, i.e. 77 for plasma and 7.4 for heart tissue.

DNR is a lipophilic molecule and thus penetrates rapidly into tissues. Therefore, normal tissue DNR levels are relatively high and may account for unfavorable side-effects [15] (Table 2). We designed a glucuronide prodrug of DNR, DNR-GA3, to be specifically activated by  $\beta$ -glucuronidase. *In vitro*, the cellular uptake was low and the octanol/phosphate-buffered saline ratio was high [7], indicating the hydrophilic nature of DNR-GA3. This will prevent rapid diffusion into cells. Indeed, after administration of DNR-GA3 to nude mice bearing human tumor xenografts, peak plasma concentrations of DNR-GA3 were very high, and the compound was rapidly cleared from the plasma, tumor, and normal tissues. The rapid clearance of the prodrug may be explained by a smaller distribution volume when compared to that of DNR, caused by its low tissue penetration.

In plasma and other normal tissues, the concentrations of DNR were lower after DNR-GA3 administration than after injection of DNR itself. As a consequence, the AUCs after DNR were much higher than after DNR-GA3 injection. In contrast, in OVCAR-3 xenografts higher concentrations of DNR from DNR-GA3 were detectable than after administration of DNR. Presumably, DNR-GA3 was activated by  $\beta$ -glucuronidase present in tumor tissue in the extracellular space, but not in normal tissues.

In human  $\beta$ -glucuronidase, it has been demonstrated that enzyme levels are elevated in tumor tissue when compared to normal tissues [16]. Enzyme levels are very low in plasma [17]. In intact mammalian cells,  $\beta$ -glucuronidase is localized inside lysosomes and microsomes [18]. Bosslet *et al.* [19] and Schumacher *et al.* [20] have shown that the enzyme is released in the extracellular space as a result of necrosis in tumors. In this way,  $\beta$ -glucuronidase can activate the prodrug DNR-GA3 specifically at the tumor site. DNR-GA3 induced a better tumor growth inhibition in larger tumors compared to small tumors [9], most likely on the basis of more necrosis. The low AUCs for DNR in the plasma and other tissues and the high AUCs for DNR in tumor tissue indicated that DNR was readily formed in the

tumor as a result of prodrug activation (Table 3). A2780 tumors had the lowest concentration of active  $\beta$ -glucuronidase, which may account for the lower AUC for DNR after DNR-GA3 administration (Table 2, Fig. 5). It is of interest that little DNR was measured in the plasma, suggesting that leakage of DNR from tumor tissue to the circulation was limited. DNR was well retained in tumor tissue, either as a result of rapid diffusion into tumor cells or retention in the necrotic areas. Prolonged exposure of tumor tissue to the DNR released from the prodrug resulted in an extended period of growth inhibition in the three xenografts that were sensitive to DNR.

In FMa tumor tissue, the AUC of DNR from DNR-GA3 was comparable to that of OVCAR-3 and MRI-H-207 tumor tissue. Despite this high AUC, no growth inhibition was seen, indicating intrinsic resistance against DNR. In DNR-sensitive A2780 xenografts, however, a relatively low AUC of DNR from DNR-GA3 was more effective than DNR itself.

In conclusion, DNR-GA3 is a non-toxic prodrug that is specifically activated to DNR in tumor tissue containing  $\beta$ -glucuronidase released by necrotic cells. In our human ovarian cancer xenografts, we have demonstrated that DNR-GA3 has a higher therapeutic index than DNR (Table 1), exemplified by a DTI of 77 for plasma and 7.4 for heart. These results with a DNR prodrug are encouraging and have led to the synthesis of an analogous prodrug of doxorubicin: DOX-GA3. Because solid tumor types are preferably treated with doxorubicin, we anticipate that this prodrug may have a broader application in the treatment of cancer.

---

*This work was supported by the Dutch Cancer Society.*

---

## References

1. Sinhababu AK and Thakker DR, Prodrugs of anticancer agents. *Adv Drug Deliv Rev* **19**: 241–273, 1996.
2. Carl PL, Chakraverty PK, Katzenellenbogen JA and Weber MJ, Protease-activated “prodrugs” for cancer chemotherapy. *Proc Natl Acad Sci USA* **77**(4): 2224–2228, 1980.

3. Deprez-de Campeneere D, Baurain R and Trouet A, Accumulation and metabolism of new anthracycline derivatives in the heart after IV injection into mice. *Cancer Chemother Pharmacol* **8**: 193–197, 1982.
4. Boven E, Hendriks HR, Erkelens CAM and Pinedo HM, The anti-tumour effects of the prodrugs N-L-leucyl-doxorubicin and vinblastine-isoleucinate in human ovarian cancer xenografts. *Br J Cancer* **66**: 1044–1047, 1992.
5. De Jong J, Geijssen GJ, Munnikma CN, Vermorken JB and Van der Vijgh WJF, Plasma pharmacokinetics and pharmacodynamics of a new prodrug N-L-leucyldoxorubicin and its metabolites in a phase I clinical trial. *J Clin Oncol* **10**: 1897–1906, 1992.
6. Haisma HJ, Boven E, Van Muijen M, De Jong J, Van der Vijgh WJF and Pinedo HM, A monoclonal antibody- $\beta$ -glucuronidase conjugate as activator of the prodrug epirubicin-glucuronide for specific treatment of cancer. *Br J Cancer* **66**: 474–478, 1992.
7. Houba PHJ, Leenders RGG, Boven E, Scheeren JW, Pinedo HM and Haisma HJ, Characterization of novel anthracycline prodrugs activated by human  $\beta$ -glucuronidase for use in antibody-directed enzyme prodrug therapy. *Biochem Pharmacol* **52**: 455–463, 1996.
8. Leenders RGG, Gerrits KAA, Ruijtenbeek R, Scheeren HW, Haisma HJ and Boven E,  $\beta$ -Glucuronyl carbamate-based pro-moieties designed for prodrugs in ADEPT. *Tetrahedron Lett* **36**: 1701–1704, 1995.
9. Houba PHJ, Boven E, Leenders RGG, Pinedo HM and Haisma HJ, The efficacy of the anthracycline prodrug daunorubicin-GA3 in human ovarian cancer xenografts. *Br J Cancer* **78**: 1600–1606, 1998.
10. Molthoff CFM, Calame JJ, Pinedo HM and Boven E, Human ovarian cancer xenografts in nude mice: characterization and analysis of antigen expression. *Int J Cancer* **47**: 72–79, 1991.
11. De Jong J, Guerand WS, Schoofs PR, Bast A and Van der Vijgh WJF, Simple and sensitive quantification of anthracyclines in mouse atrial tissue using high-performance liquid chromatography and fluorescence detection. *J Chromatogr* **570**: 209–216, 1991.
12. Haisma HJ, van Muijen M, Pinedo HM and Boven E, Comparison of two anthracycline-based prodrugs for activation by a monoclonal antibody- $\beta$ -glucuronidase conjugate in the specific treatment of cancer. *Cell Biophysics* **24/25**: 185–192, 1994.
13. Boven E, De Jong J, Kuiper CM, Bast A and Van der Vijgh WJF, Relationship between the tumour pharmacokinetics and the antiproliferative effects of anthracyclines and their metabolites. *Eur J Cancer* **32A**: 1382–1387, 1996.
14. Kearney AS, Prodrugs and targeted drug delivery. *Adv Drug Del Rev* **19**: 225–239, 1996.
15. Cusack BJ, Young SP and Olson RD, Daunorubicin and daunorubicinol pharmacokinetics in plasma and tissues in the rat. *Cancer Chemother Pharmacol* **35**: 231–218, 1995.
16. Connors TA and Whisson ME, Cure of mice bearing advanced plasma cell tumours with aniline mustard: the relationship between glucuronidase activity and tumour sensitivity. *Nature* **210**: 866–867, 1966.
17. Fishman WH, *Metabolic conjugation and metabolic hydrolysis*. Academic Press, New York, London, 1970.
18. Levvy GA and Conchie J,  $\beta$ -glucuronidase and the hydrolysis of glucuronides. In: *Glucuronic Acid, Free and Combined* (Ed. Dutton GJ), pp. 301–364. Academic Press, New York, 1966.
19. Bosslet K, Czech J and Hoffman D, A novel one-step tumor-selective prodrug activation system. *Tumor Targeting* **1**: 45–50, 1995.
20. Schumacher U, Adam E, Zangemeister-Wittke U and Gossrau R, Histochemistry of therapeutically relevant enzymes in human tumours transplanted into severe combined immunodeficient (SCID) mice: nitric oxide synthase-associated diaphorase,  $\beta$ -D-glucuronidase and non-specific alkaline phosphatase. *Acta Histochem* **98**: 381–387, 1996.